

# Ultrasonic study of the temperature and pressure dependences of the elastic properties of a single-crystal Heusler structure $\text{Cu}_{41}\text{Mn}_{20}\text{Al}_{39}$ alloy

G. A. SAUNDERS, H. J. LIU

*School of Physics, University of Bath, Bath BA2 7AY, UK*

M. CANKURTARAN

*Hacettepe University, Department of Physics, Beytepe, 06532 Ankara, Turkey*

H. BACH

*Kristall-lab, Institut Für Experimentalphysik, Ruhr-Universität Bochum, Germany*

Pulse-echo-overlap measurements of ultrasonic wave velocity have been used to determine the elastic-stiffness tensor components  $C_{ij}$  and the adiabatic bulk modulus,  $B^S$ , of a ferromagnetic Heusler structure  $\text{Cu}_{41}\text{Mn}_{20}\text{Al}_{39}$  at % alloy single crystal as functions of temperature in the range 14–300 K and hydrostatic pressure up to 0.2 GPa at room temperature. At 295 K the elastic stiffnesses are:  $C_{11} = 133$  GPa,  $C_{44} = 92$  GPa,  $C'$  ( $= (C_{11} - C_{12})/2$ ) = 17 GPa,  $C_{12} = 99$  GPa,  $C_L$  ( $= C_{11} + C_{44} - C'$ ) = 205 GPa, and  $B^S$  ( $= C_{11} - 4C'/3$ ) = 106 GPa.  $\text{Cu}_{41}\text{Mn}_{20}\text{Al}_{39}$  is a comparatively soft material elastically because its elastic properties are influenced strongly by magnetoelastic effects. The results of measurements of the effects of hydrostatic pressure on the ultrasonic wave velocity have been used to obtain the hydrostatic-pressure derivatives of the elastic-stiffness tensor components. At 295 K  $(\partial C_{11}/\partial P)_{P=0}$ ,  $(\partial C_{44}/\partial P)_{P=0}$ ,  $(\partial C'/\partial P)_{P=0}$ ,  $(\partial C_{12}/\partial P)_{P=0}$ ,  $(\partial C_L/\partial P)_{P=0}$ , and  $(\partial B^S/\partial P)_{P=0}$  are  $5.0 \pm 0.1$ ,  $3.0 \pm 0.1$ ,  $1.0 \pm 0.2$ ,  $3.0 \pm 0.3$ ,  $7.7 \pm 0.4$  and  $3.7 \pm 0.4$ , respectively. Application of hydrostatic pressure does not induce acoustic-mode softening; the pressure derivatives  $(\partial C_{ij}/\partial P)_{P=0}$  and  $(\partial B^S/\partial P)_{P=0}$  and the acoustic-mode Grüneisen parameters are positive. An interesting feature of the non-linear acoustic behaviour of this alloy is that the value obtained for  $(\partial C'/\partial P)_{P=0}$ , associated with the softer shear mode propagated along the [110] direction and polarized along the [110] direction, is small in comparison with those of the other shear and longitudinal modes. The Grüneisen parameter of this mode, and hence its vibrational anharmonicity, is much larger than those of the other long-wavelength acoustic phonon modes. © 1998 Kluwer Academic Publishers

## 1. Introduction

Magnetoelastic effects can have important ramifications in the elastic properties of ferromagnetic three-dimensional alloys, prompting an ultrasonic study of the effects of temperature and hydrostatic pressure on the elastic behaviour of monocrystalline, ferromagnetic Heusler alloy,  $\text{Cu}_{41}\text{Mn}_{20}\text{Al}_{39}$  at % alloy. Previously the elastic-stiffness moduli of a single-crystal  $\text{Cu}_2\text{MnAl}$  Heusler alloy have been measured at room temperature [1] and in the temperature range 77–295 K at atmospheric pressure [2]; the alloy  $\text{Cu}_{41}\text{Mn}_{20}\text{Al}_{39}$  studied here differs markedly in composition but the Heusler alloy structure has a wide existence range. In the present work ultrasonic wave velocity measurements have been made down to 14 K. The effects of pressure on the elastic behaviour of copper-manganese-aluminum alloys, including those with compositions in the range that have the Heusler structure, are unknown. To establish the non-linear

acoustic properties of  $\text{Cu}_{41}\text{Mn}_{20}\text{Al}_{39}$ , ultrasonic wave velocities have been measured as a function of hydrostatic pressure up to 0.2 GPa at room temperature. The outcome of this experimental work has been the determination of each of the independent second-order elastic-stiffness tensor components and related elastic properties and how they vary with temperature and pressure. The present results provide intriguing physical insight into the elastic and non-linear acoustic properties of  $\text{Cu}_{41}\text{Mn}_{20}\text{Al}_{39}$  – part of a programme of experimental investigation of magnetoelasticity in three-dimensional ordered alloys and compounds.

## 2. Experimental procedure

Alloy single crystals were grown by a Czochralski method from a levitated melt that is described elsewhere [3]. The crystal was grown by a lowering through the melting point (1223 K) at a pulling rate of

3 mm h<sup>-1</sup>, 60 rotations min<sup>-1</sup>, in an Ar atmosphere of 1.05 kPa. It was not subjected to a subsequent annealing procedure. The sample used for ultrasonic measurements was homogeneous, with a mosaicity of about 1°. The crystal quality of this cubic material was examined by taking Laue back-reflection photographs along the boule; it has the Heusler alloy structure. Microprobe examination scans around the crystal showed that its composition was within ±1 at % of Cu<sub>41</sub>Mn<sub>20</sub>Al<sub>39</sub> using energy dispersive X-ray microanalysis. The crystal was orientated to ±0.5° on a three-arc goniometer using Laue back-reflection photography. A sample in the shape of a parallelepiped with dimensions 6.255, 6.349 and 6.504 mm<sup>3</sup>, which was large enough for precision measurements of ultrasonic wave velocities, was cut and polished with faces, normal to the [001] and [110] crystallographic axes, flat to surface irregularities of about 3 μm and parallel to better than 10<sup>-3</sup> rad.

To generate and detect ultrasonic pulses, X- and Y-cut (for longitudinal and shear waves, respectively) 10-MHz quartz transducers were bonded to the specimen using Nonaq stopcock grease for low-temperature experiments. Dow resin was used as the bonding material for high-pressure experiments. With the exception of the C' mode, whose ultrasonic wave velocity under pressure was measured in a saturation magnetic field of 1.2 T (see Section 3.2.), ultrasonic experiments were carried out in the absence of a magnetic field. Ultrasonic pulse transit times were measured using a pulse-echo-overlap system [4], capable of resolution of velocity changes to 1 part in 10<sup>5</sup> and particularly well suited to determination of pressure- or temperature-induced changes in velocity. The temperature dependence of ultrasound velocity was measured between 14 and 300 K using a closed-cycle cryostat. The dependence of ultrasonic wave velocity upon hydrostatic pressure was measured at room temperature. Hydrostatic pressure up to 0.2 GPa was applied in a piston-and-cylinder apparatus using sili-

cone oil as the pressure-transmitting medium. Pressure was measured using a pre-calibrated manganin resistance gauge. Pressure-induced changes in the sample dimensions were accounted for by using the "natural velocity (*W*)" technique [5, 6].

### 3. Results

#### 3.1. Temperature dependence of the elastic–stiffness tensor components

The adiabatic elastic–stiffness components,  $C_{11}$ ,  $C_{44}$ ,  $C'$  [ $= (C_{11} - C_{12})/2$ ],  $C_{12}$  and  $C_L (= C_{11} + C_{44} - C')$ ; the adiabatic bulk modulus,  $B^S (= C_{11} - 4C'/3)$ ; the elastic Debye temperature,  $\Theta_D^{el}$ ; and the elastic anisotropy ratio,  $A (= C_{44}/C')$ , determined at room temperature and atmospheric pressure from the ultrasonic velocity data and sample density (6490 kg m<sup>-3</sup>), are given in Table I. The results obtained for the elastic stiffnesses of Cu<sub>41</sub>Mn<sub>20</sub>Al<sub>39</sub> are similar to those reported for a Cu<sub>2</sub>MnAl Heusler alloy crystal [2] and Cu<sub>2-x</sub>Mn<sub>1-x</sub>Al alloys ( $x = 0.8, 0.7$  and  $0.6$ ) [7]. The value determined for  $\Theta_D^{el}$  is substantially higher than that ( $= 330$  K) deduced from low-temperature specific-heat data for a Heusler alloy of composition Cu<sub>0.484</sub>Mn<sub>0.24</sub>Al<sub>0.276</sub> [8]. The Cu<sub>41</sub>Mn<sub>20</sub>Al<sub>39</sub> alloy studied here has a large value of 5.4 for the elastic anisotropy ratio. Micheluti *et al.* [2] obtained a strong elastic anisotropy in their Cu<sub>2</sub>MnAl crystal (Table I), which accounted for the large anisotropy observed in the magnetostriction coefficients. Although the magnetocrystalline anisotropy of Cu<sub>2</sub>MnAl was found to be very small, being two orders of magnitude smaller than that of nickel, the magnetoelastic contribution to the observed magnetic anisotropy was significant [2].

In ferromagnetic and antiferromagnetic three-dimensional alloys the elastic–stiffness tensor component,  $C_{11}$  (and the bulk modulus), are often small compared with those of the parent elements; this is also true for  $C_L$ , which corresponds to a longitudinal

TABLE I The elastic and non-linear acoustic properties of the ferromagnetic Cu<sub>41</sub>Mn<sub>20</sub>Al<sub>39</sub> alloy determined at room temperature and atmospheric pressure in comparison with those of other Mn alloys

Description	Cu <sub>41</sub> Mn <sub>20</sub> Al <sub>39</sub>	Cu <sub>2</sub> MnAl (from [2])	Ni <sub>2</sub> MnGa (from [16])	Mn <sub>73</sub> Ni <sub>27</sub> (from [10])	Mn <sub>78</sub> Pt <sub>22</sub> (from [11])
elastic-stiffness components,					
$C_{11}$ (GPa)	133 ± 1	135.8	136 ± 3	129	94.2
$C_{44}$ (GPa)	92 ± 1	93.9	102 ± 3	98	84.7
$C'$ [ $= (C_{11} - C_{12})/2$ ] (GPa)	17 ± 2	–	22 ± 2	26	29.2
$C_{12}$ (GPa)	99 ± 2	–	–	77	35.8
$C_L$ [ $= (C_{11} + C_{44} - C')/2$ ] (GPa)	205 ± 3	210.0	222 ± 9	201	149.7
Bulk modulus, $B^S$ , GPa	106 ± 4	–	–	94	55.2
Debye temperature, $\Theta_D^{el}$ , K	393	376	–	–	–
Anisotropy ratio, $C_{44}/C'$	5.4	4.9	–	–	–
$(\partial C_{11}/\partial P)_{P=0}$	5.0 ± 0.1	–	–	5.2	6.2
$(\partial C_{44}/\partial P)_{P=0}$	3.0 ± 0.1	–	–	3.5	4.3
$(\partial C'/\partial P)_{P=0}$	1.0 ± 0.2	–	–	0.9	1.0
$(\partial C_{12}/\partial P)_{P=0}$	3.0 ± 0.3	–	–	3.2	4.5
$(\partial C_L/\partial P)_{P=0}$	7.7 ± 0.4	–	–	7.7	9.5
$(\partial B^S/\partial P)_{P=0}$	3.7 ± 0.4	–	–	3.9	4.8
Mean acoustic Grüneisen parameter, $\gamma^{el}$	1.9 ± 0.2	–	–	1.59	1.35

wave-propagated along a  $\langle 110 \rangle$  direction [9]. Ferromagnetic  $\text{Cu}_{41}\text{Mn}_{20}\text{Al}_{39}$  also shows long-wavelength longitudinal acoustic phonons that are relatively soft and a comparatively small bulk modulus. There is striking similarity between the values of elastic stiffness  $C_{ij}$  obtained for the  $\text{Cu}_{41}\text{Mn}_{20}\text{Al}_{39}$  alloy and those measured for antiferromagnetic  $\text{Mn}_{73}\text{Ni}_{27}$  and  $\text{Mn}_{78}\text{Pt}_{22}$  alloys [10, 11], see Table I. The longitudinal acoustic-mode softening due to the magnetovolume interaction, which results in a small value for  $C_{11}$ , can be instrumental in reducing  $C' [= (C_{11} - C_{12})/2]$  in turn. An important feature of this ferromagnetic  $\text{Cu}_{41}\text{Mn}_{20}\text{Al}_{39}$  alloy is the very small value of shear stiffness,  $C'$  associated with the ultrasonic waves propagated along the  $[110]$  direction and polarized along the  $[1\bar{1}0]$  direction: this shear mode is markedly soft. A small value of the shear stiffness,  $C'$ , enabled  $\{110\}$  slip in a single-crystal alloy with composition  $\text{Cu}_{52.3}\text{Mn}_{22.7}\text{Al}_{25.0}$  [1, 12]. A very low value and a softening of the shear stiffness,  $C'$ , with decreasing temperature have been found in  $\beta$ -phase  $\text{AuCuZn}_2$  [13],  $\text{Cu}_{2+x}\text{Mn}_{1-x}\text{Al}$  alloys ( $x = 0.8, 0.7$  and  $0.6$ ) [7], and ferromagnetic  $\text{Ni}_2\text{MnGa}$  alloy [14–16].

A small value of  $C'$  often implies a lattice instability against the soft shear acoustic phonons propagating in the  $[110]$  direction and polarized parallel to the  $[1\bar{1}0]$  direction, which can lead to a displacive phase transition [13, 17]. This occurs in the ferromagnetic  $\text{Ni}_2\text{MnGa}$  alloy, which undergoes a martensitic phase transition from the  $L2_1$  structure to a modulated crystal structure having an approximately tetragonal symmetry [14–16]. Ultrasonic wave velocity measurements as a function of temperature have revealed a pronounced dip in the value of  $(C_{11} - C_{12})/2$  in the vicinity of the martensitic transition temperature [16].

The temperature dependences of the adiabatic elastic stiffness  $C_{11}$ ,  $C_L$ , and  $C_{44}$  are shown in Fig. 1. They were obtained from the sample density and the velocities of ultrasonic waves propagated along the  $[001]$  and  $[110]$  directions of the  $\text{Cu}_{41}\text{Mn}_{20}\text{Al}_{39}$  crystal as it was cooled from 300 K down to 14 K. Corrections for changes in sample length and density have not been made because the thermal expansion of this alloy has not been measured; however, the corrections on elastic moduli are not expected to be greater about 1%. The longitudinal  $C_{11}$  and  $C_L$  and the shear  $C_{44}$  elastic stiffnesses increases smoothly with decreasing temperature and do not show any pronounced unusual effects. These elastic moduli increase steadily in the usual way, as the temperature is decreased to about 100 K and then level off with a progressively decreasing slope. There was no thermal hysteresis in the elastic moduli of the three modes and no irreversible effects, when the alloy was cycled between room temperature and 14 K. This indicates that decomposition or phase precipitation do not occur in this temperature range [7, 18]. The Curie temperature of this alloy is sufficiently high ( $\sim 600$  K), that any effects of the magnetic transition on the temperature dependence of  $C_{ij}$  in the range below 300 K can be neglected. The value of  $C'$  increases approximately linearly with decreasing temperature from 300 K down to 14 K,

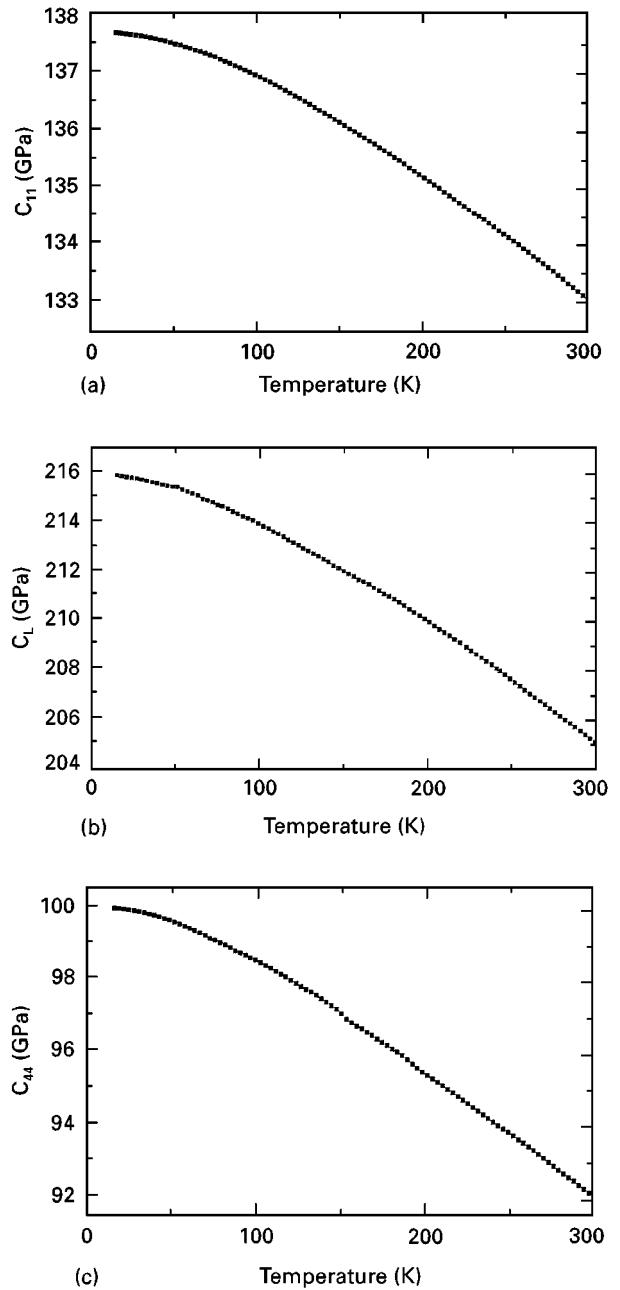


Figure 1 Temperature dependences of the adiabatic elastic-stiffness tensor components. (a)  $C_{11}$ , (b)  $C_L (= C_{11} + C_{44} - C')$ , and (c)  $C_{44}$  of the  $\text{Cu}_{41}\text{Mn}_{20}\text{Al}_{39}$  single crystal.

and the average temperature gradient is very small:  $(\partial C'/\partial T)_{P=0} = -0.0064 \text{ GPa K}^{-1}$ .

### 3.2. Hydrostatic-pressure dependences of the ultrasonic wave velocities and elastic stiffness components

The ultrasonic wave velocities associated with the longitudinal  $C_{11}$  and  $C_L$  and the shear  $C_{44}$  and  $C'$  modes increase approximately linearly with pressure (Fig. 2). The pressure dependence of the velocity of the  $C'$  mode was measured in a saturation magnetic field of 1.2 T parallel to the wave propagation direction, which substantially improved the pulse-echo train of this highly attenuated mode and allowed satisfactory measurements to be made. The data for all modes are

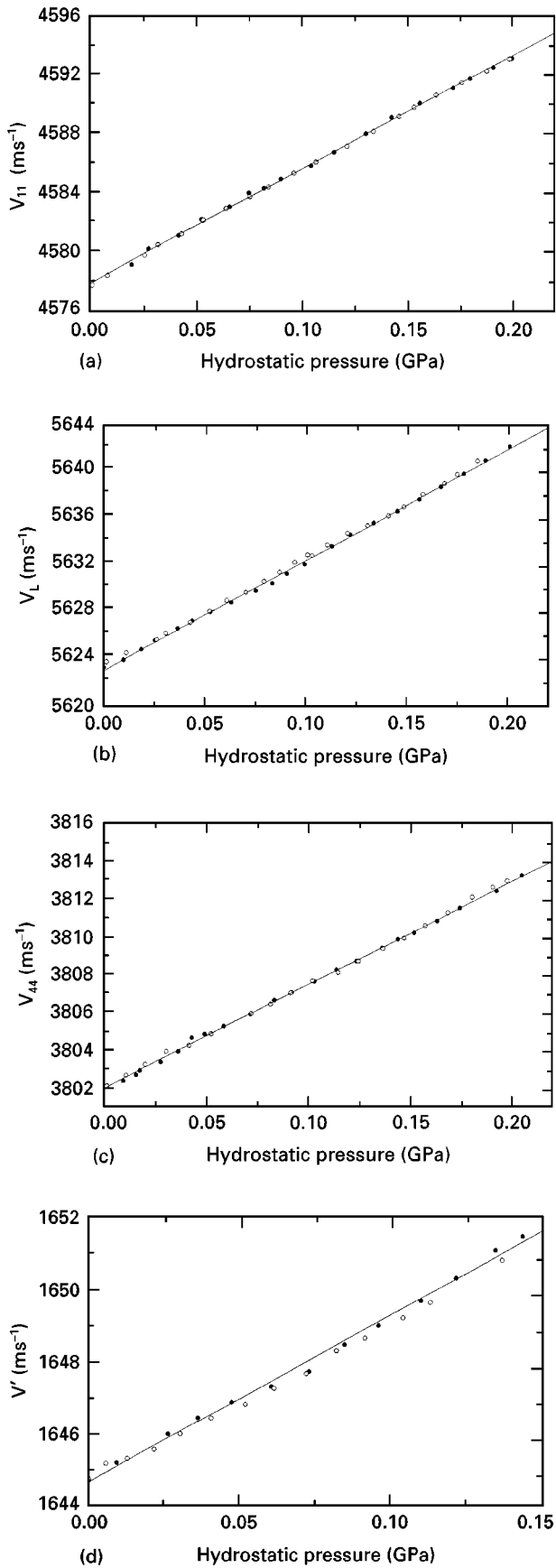


Figure 2 Hydrostatic-pressure dependences of the velocities of 10-MHz ultrasonic waves in the  $\text{Cu}_{41}\text{Mn}_{20}\text{Al}_{39}$  alloy at room temperature: (a) longitudinal mode propagated along the [001] direction, (b) longitudinal mode propagated along the [110] direction, (c) polarized shear mode propagated along the [001] direction, and (d) [110] polarized shear mode propagated along the [110] direction (measured in a magnetic field of 1.2 T): ● measurements made with increasing pressure, (○) data measured as the pressure was decreased.

reproducible under pressure cycling and show no measurable hysteresis effects. This observation indicates that the  $\text{Cu}_{41}\text{Mn}_{20}\text{Al}_{39}$  crystal does not alter under pressure cycling up to 0.2 GPa at room temperature and there is no relaxation of any residual stress. The hydrostatic-pressure derivatives  $(\partial C_{ij}/\partial P)_{P=0}$  of the elastic-stiffness tensor components have been obtained from the ultrasonic velocity measurements under pressure by using [6]

$$\left(\frac{\partial C_{ij}}{\partial P}\right)_{P=0} = (C_{ij})_{P=0} \left(\frac{2f'}{f_0} + \frac{1}{3B^T}\right)_{P=0} \quad (1)$$

where  $B^T$  is the isothermal bulk modulus,  $f_0$  is the pulse-echo-overlap frequency at atmospheric pressure and  $f'$  is its pressure derivative. In the absence of thermal expansion and specific-heat data,  $B^S$  has been used rather than  $B^T$  throughout the calculations, a procedure that introduces only a negligible error. The hydrostatic-pressure derivatives  $(\partial C_{ij}/\partial P)_{P=0}$ , in the zero pressure limit, of this ferromagnetic  $\text{Cu}_{41}\text{Mn}_{20}\text{Al}_{39}$  alloy all have positive values (Table I). The elastic stiffnesses and thus the slopes of the acoustic-mode dispersion curves, at the long-wavelength limit, increase with pressure in the normal way. The application of pressure to  $\text{Cu}_{41}\text{Mn}_{20}\text{Al}_{39}$  does not induce acoustic-mode softening. The values obtained for  $(\partial C_{ij}/\partial P)_{P=0}$  of  $\text{Cu}_{41}\text{Mn}_{20}\text{Al}_{39}$  are similar to those found for face centred cubic (f.c.c.) Mn–Ni and Mn–Pt alloys (Table I). The pressure derivatives of the elastic stiffness of  $\text{Cu}_{41}\text{Mn}_{20}\text{Al}_{39}$  follow the common trend found for cubic crystals  $(\partial C_{11}/\partial P)_{P=0} > (\partial C_{44}/\partial P)_{P=0} > (\partial C'/\partial P)_{P=0}$ . The largest pressure derivative is  $(\partial C_{11}/\partial P)_{P=0}$  implying that the higher-order elastic effects are dominated by nearest-neighbour repulsive forces. It should be noted that the value obtained for  $(\partial C'/\partial P)_{P=0}$  is very small in comparison with those of the other shear and longitudinal modes, again emphasizing the fact that the shear mode propagated in the [110] direction and polarized along the [110] direction is markedly soft, although it does not soften further under pressure or when temperature is lowered.

The measurements of the elastic stiffnesses and their hydrostatic-pressure derivatives have been used to calculate the volume compression,  $V(P)/V_0$ , of  $\text{Cu}_{41}\text{Mn}_{20}\text{Al}_{39}$  up to very high pressures, using an extrapolation method based on the Murnaghan equation of state in the logarithmic form [19]. The calculation has been performed at room temperature and results are shown in Fig. 3. The comparatively large magnitude of the volume compression for  $\text{Cu}_{41}\text{Mn}_{20}\text{Al}_{39}$  is typical of that for three-dimensional transition-metal alloys containing Mn, in which the magnetoelastic interaction reduces the bulk modulus [11].

### 3.3. Grüneisen parameters and acoustic-mode vibrational anharmonicity

Properties of a solid that depend upon thermal motion of the atoms are much influenced by anharmonicity. It is usual to describe the anharmonic properties in terms of Grüneisen parameters, which

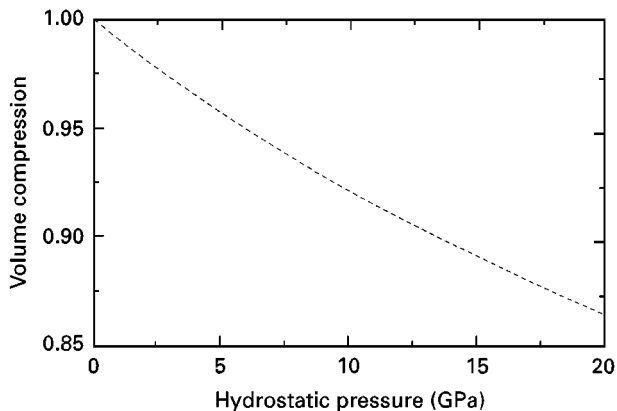


Figure 3 Volume compression of  $\text{Cu}_{41}\text{Mn}_{20}\text{Al}_{39}$  at room temperature extrapolated to very high pressures using Murnaghan's [19] equation of state.

quantify the volume or strain dependence of the lattice vibrational frequencies. The dependence of the acoustic-mode frequency,  $\omega_p$ , in a phonon branch,  $p$ , on volume  $V$ , can be expressed as a mode Grüneisen parameter

$$\gamma_p = - \left[ \frac{\partial(\ln \omega_p)}{\partial(\ln V)} \right]_{P=0} \quad (2)$$

which can be obtained from the measurements of  $C_{IJ}$  and  $(\partial C_{IJ}/\partial P)_{P=0}$ . The acoustic-mode Grüneisen parameters of  $\text{Cu}_{41}\text{Mn}_{20}\text{Al}_{39}$  at 295 K, calculated using the equations developed by Brugger and Fritz [20], are shown in Fig. 4 as a function of propagation direction. Both longitudinal and shear mode  $\gamma$  are positive. The Grüneisen parameters for the longitudinal and quasi-longitudinal modes are almost independent of propagation direction. However, the Grüneisen parameter associated with the soft shear mode propagated along the [110] direction and polarized along the  $[1\bar{1}0]$  direction is substantially larger than that of the longitudinal modes; this is an anomalous behaviour resulting from large vibrational anharmonicity, a common feature in materials in which the shear stiffness,  $C'$ , is small.

The mean acoustic Grüneisen parameter,  $\gamma^{\text{el}}$ , which is a measure of the overall contribution of zone-centre acoustic modes to the lattice vibrational anharmonicity, has been calculated by summing all of the long-wavelength acoustic-mode Grüneisen parameters with the same weight for each mode using

$$\gamma^{\text{el}} = \sum_{p=1}^3 \int_{\Omega} \gamma_p d\Omega / 3 \int_{\Omega} d\Omega \quad (3)$$

where the integration is over the whole space,  $\Omega$ . A value of 1.9 has been obtained for  $\gamma^{\text{el}}$  of  $\text{Cu}_{41}\text{Mn}_{20}\text{Al}_{39}$  in accord with that of many three-dimensional cubic crystals (see for instance [9]). The thermal Grüneisen parameter  $\gamma^{\text{th}}$  ( $= \alpha V B^S / C_p$ ) cannot be calculated because the thermal expansion,  $\alpha$ , and specific heat,  $C_p$ , data are not yet available.

In ferromagnetic crystals there is a contribution to the total energy arising from the interatomic magnetic

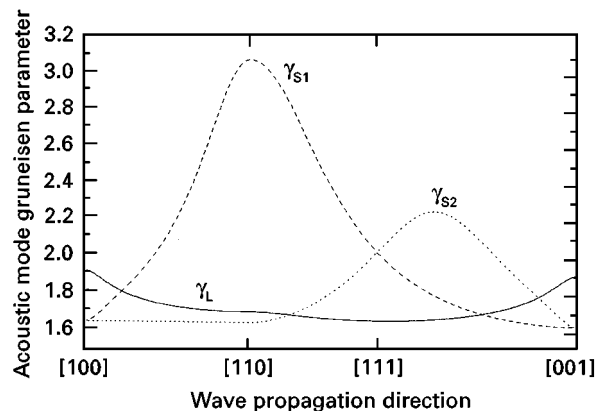


Figure 4 Long-wavelength longitudinal (—) and shear (---, ...) acoustic-mode Grüneisen parameters as a function of mode propagation direction for  $\text{Cu}_{41}\text{Mn}_{20}\text{Al}_{39}$  at room temperature.

interactions between the aligned magnetic moments. Because the elastic-stiffness tensor components,  $C_{IJ}$ , are directly related to the second derivatives of the free energy with respect to strain, they include an intrinsic contribution due to magnetic ordering. The hydrostatic-pressure derivatives,  $(\partial C_{IJ}/\partial P)_{P=0}$ , of the elastic stiffness moduli are related to the third derivatives of the free energy, and hence to the vibrational anharmonicity of the long-wavelength acoustic phonons, and so the acoustic-mode Grüneisen parameters also include magnetoelastic contributions, which play an important role in the determination of the elastic and non-linear acoustic properties shown by this ferromagnetic alloy.

#### 4. Conclusions

The velocities of pure ultrasonic modes propagated along the [001] and [110] directions of ferromagnetic  $\text{Cu}_{41}\text{Mn}_{20}\text{Al}_{39}$  single crystal have been measured as functions of temperature and hydrostatic pressure. There are several interesting features to note, which shed light on the elastic and non-linear acoustic and lattice dynamical properties of this alloy. They can be summarized as follows:

1. The  $\text{Cu}_{41}\text{Mn}_{20}\text{Al}_{39}$  alloy is a comparatively soft material elastically. Its volume-dependent elastic stiffnesses  $C_{11}$  and  $C_L$ , and the bulk modulus,  $B^S$ , are small in comparison with those of three-dimensional transition-metal elements. The elastic properties are influenced strongly by magnetoelastic effects.
2. The value of the shear elastic stiffness,  $C'$  [ $= (C_{11} - C_{12})/2$ ], associated with the ultrasonic waves propagated along the [110] direction and polarized along the  $[1\bar{1}0]$  direction, is small; this shear mode is markedly soft. In consequence the elastic anisotropy ratio is large.
3. The hydrostatic-pressure derivatives,  $(\partial C_{IJ}/\partial P)_{P=0}$ , of the elastic stiffness and  $(\partial B^S/\partial P)_{P=0}$  of the bulk modulus have positive values. Application of pressure does not induce acoustic-mode softening. Nevertheless, the value found for  $(\partial C'/\partial P)_{P=0}$  is very small in comparison with those of the other shear and longitudinal modes.

4. The long-wavelength acoustic-mode Grüneisen parameters at room temperature have normal values but significantly are large in the branch that includes the soft  $C'$  mode, which therefore exhibits a high vibrational anharmonicity.

### Acknowledgements

We are grateful to NATO (Scientific and Environmental Affairs Division, Grant number CRG960584) and the Deutsche Forschungsgemeinschaft (SFB166) for financial support. We would also like to thank E. F. Lambson and W. A. Lambson for technical assistance. One of us (MC) would also like to thank the British Council, Ankara for a grant-in-aid.

### References

1. M. L. GREEN, G. Y. CHIN and J. B. VANDERSANDE, *Metall. Trans.* **8A** (1977) 353.
2. B. MICHELUTTI, R. PERRIER DE LA BATHIE, E. DU TREMOLET DE LACHEISSERIE and A. WAIN TAL, *Solid State Commun.* **25** (1978) 163.
3. P. STAUCHE, S. ERDT-BÖHM, H. BRINKMANN and H. BACH, *J. Cryst. Growth* **166** (1996) 390.
4. E. P. PAPADAKIS, *J. Acoust. Soc. Amer.* **42** (1967) 1045.
5. R. N. THURSTON and K. BRUGGER, *Phys. Rev.* **133** (1964) A1604.
6. R. N. THURSTON, *Proc. IEEE* **53** (1965) 1320.
7. A. PRASETYO, F. REYNAUD and H. WARLIMONT, *Acta Metall.* **24** (1976) 651.
8. N. G. FENANDER, L. WIKTORIN and H. P. MYERS, *J. Phys. Chem. Solids* **29** (1968) 1973.
9. G. A. SAUNDERS, D. BALL, M. CANKURTARAN, Q. WANG, E. ARNSCHEIDT, C. JACOBS, F. IMBIERWITZ, J. PELZL and H. BACH, *Phys. Rev. B* **55** (1997) 11 181.
10. G. A. SAUNDERS and M. D. SALEH, *Philos. Mag. B* **68** (1993) 437.
11. G. A. SAUNDERS, M. CANKURTARAN, P. RAY, J. PELZL and H. BACH, *Phys. Rev. B* **48** (1993) 3216.
12. Y. UMAKOSHI, M. YAMAGUCHI and T. YAMANE, *Acta Metall.* **32** (1984) 649.
13. S. KASHIDA and H. KAGA, *J. Phys. Soc. Jpn* **42** (1977) 499.
14. A. N. VASIL'EV, V. V. KOKORIN, YU. I. SAVCHENKO and V. A. CHERNENKO, *Sov. Phys. JETP* **71** (1990) 803.
15. J. WORGUL, E. PETTI and J. TRIVISONNO, *Phys. Rev. B* **54** (1996) 15 695.
16. LL. MAÑOSA, A. GONZÀLES-COMAS, E. OBRADÓ, A. PLANES, V. A. CHERNENKO, V. V. KOKORIN and E. CESARI, *ibid.* **55** (1997) 11 068.
17. M. MORI, Y. YAMADA and G. SHIRANE, *Solid State Commun.* **17** (1975) 127.
18. R. KOZUBSKI and J. SOLTYS, *J. Mater. Sci.* **17** (1982) 1441.
19. F. D. MURNAGHAN, *Proc. Natl. Acad. Sci. USA* **30** (1944) 244.
20. K. BRUGGER and T. C. FRITZ, *Phys. Rev.* **157** (1967) 524.

*Received 11 September 1997  
and accepted 11 May 1998*